

Large Reasoning Models for 3D Floorplanning in EDA: Learning from Imperfections

Fin Amin^{*‡}

Department of Electrical

& Computer Engineering

North Carolina State University

samin2@ncsu.edu

Nirjhor Rouf

Department of Electrical

& Computer Engineering

North Carolina State University

nrouf2@ncsu.edu

Tse-Han Pan^{*}

Department of Electrical

& Computer Engineering

North Carolina State University

tpan@ncsu.edu

Md Kamal Ibn Shafi

Department of Electrical
& Computer Engineering

North Carolina State University

mibnsha@ncsu.edu

Paul D. Franzon

Department of Electrical
& Computer Engineering

North Carolina State University

paulf@ncsu.edu

Abstract—In this paper, we introduce Dreamweaver, which belongs to a new class of auto-regressive decision-making models known as large reasoning models (LRMs). Dreamweaver is designed to improve 3D floorplanning in electronic design automation (EDA) via an architecture that melds advancements in sequence-to-sequence reinforcement learning algorithms. A significant advantage of our approach is its ability to effectively reason over large discrete action spaces, which is essential for handling the numerous potential positions for various functional blocks in floorplanning. Additionally, Dreamweaver demonstrates strong performance even when trained on entirely random trajectories, showcasing its capacity to leverage sub-optimal or non-expert trajectories to enhance its results. This innovative approach contributes to streamlining the integrated circuit (IC) design flow and reducing the high computational costs typically associated with floorplanning. We evaluate its performance against a current state-of-the-art method, highlighting notable improvements.

Index Terms—decision transformers, generative reinforcement learning, floorplanning, electronic design automation

I. INTRODUCTION AND MOTIVATION

Floorplanning is the process of determining the optimal placement of functional blocks within an integrated circuit (IC) layout to meet specific design criteria such as power, performance, area, and thermal characteristics. The input to this problem typically includes a netlist, which is a description of the IC's components and the connections between them. Floorplanning is a major challenge in IC design that is pivotal in meeting the design specifications. The placement of major functional blocks can have a significant impact on the IC's power, performance, area, and thermal specifications. As a result, the quality of the floorplan is critical as poor floorplans are often expensive to fix once the subsequent physical design

processes are initiated. Exacerbating these challenges is the fact that floorplanning is an NP-hard problem [7] which will often exhibit a large search space for optimization even with a moderate number of functional blocks. These requirements on floorplan quality and scalability have motivated research on machine learning solutions to generate desirable floorplans.

Recent works that have explored the feasibility of applying reinforcement learning (RL) in mixed-macro placement have shown promising results [6], [19], [23]. The RL agents in these studies have improved productivity by reducing the placement time on top of generating layouts with competitive wirelength and congestion to work done by human experts. 2021 saw a seminal step towards the application of RL in IC design as [23] showed the feasibility of using a deep RL approach in chip floorplanning. However, this solution is plagued by a few key issues. Notably, the agent's learning becomes mired after a certain amount of time. *Chipformer* [19] reports promising results on wirelength optimization of the layout, but the scope of the study omits the floorplan impact from other design constraints, such as thermal requirements. Additionally, neither method scales well with respect to the canvas size.

This study is an attempt to address the scalability issue while improving the quality of the floorplan with additional optimization objectives. By treating floorplanning as a regression problem rather than a classification one, we achieve better results over larger action spaces as well as reducing computational costs.

Our contribution is a new class of auto-regressive models, named large reasoning models (LRMs) which are adept at reasoning over large discrete action spaces (LDAS). Due to the large action space that needs to be considered in 3D floorplanning, we find that our approach offers improvements in terms of sample efficiency compared to the existing ML state-of-the-art. To this end, we introduce Dreamweaver, the first LRM, which reasons over a *continuous action representation*. This addresses the fundamental problem of the large discrete action

^{*}This author was funded by the Qualcomm Innovation Fellowship.

[‡]This author was employed at MIT Lincoln Laboratory during the time this work was conducted independently.

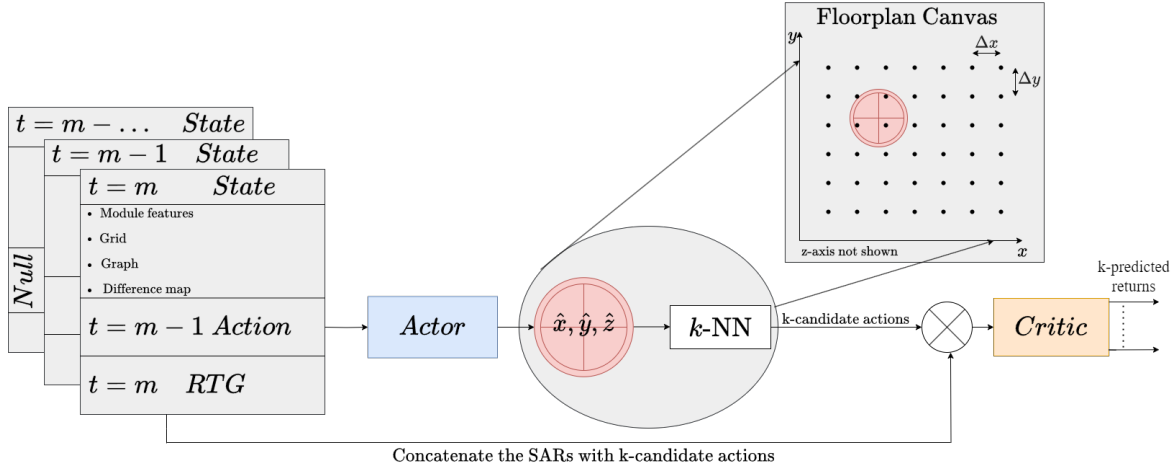


Fig. 1: Our agent melds recent advancements in auto-regressive decision models with the Wolpertinger architecture. This figure shows the flow of information across a single time-step of inferencing. First, the SARs (γ_t) are input into the actor so that the actor can propose a candidate centroid location, $\alpha = \hat{x}, \hat{y}, \hat{z}$, then, k -NN is used to find the k nearest legal actions to α . Finally, the critic produces \hat{g}_t , the return to go for the remainder of the trajectory for each of the k actions. The action which produces the best \hat{g}_t is ultimately selected in accordance with equation 1.

space encountered in floorplanning. Moreover, this work not only uses interconnect wirelength, but also explores congestion and thermal estimations as optimization objectives. Namely, we show how Dreamweaver addresses multiple objectives when considering the return of a decision.

II. BACKGROUND

Our discussion of prior work has two central themes. The first theme is an overview of existing ML-based approaches to floorplanning. The goal is to discuss their contributions along with their limitations. The second theme concerns the relevant discoveries in the field of RL and auto-regressive models which guided our algorithm design.

A. ML Solutions to Floorplanning

The classical approaches for 2D floorplanning usually leverage analytical and metaheuristic algorithms. While analytical approaches are good at finding the minimum area solutions, they scale poorly with a large number of constraints. On the other hand, metaheuristic methods are capable of handling more complex problems, however, the lack of knowledge reuse makes them quite inefficient.

The issues with the classical algorithms motivated the search for more efficient solutions; one pioneering step towards this was [23]. This work showed the feasibility of approaching the floorplanning problem from the perspective of RL. Their off-the-shelf RL algorithms while successful in implementation are not well-optimized. Their agent learns slowly despite high computational resources. Another RL approach for floorplanning [28] represents the floorplan using sequence pairs. This work compares one random solution with another and iteratively chooses the best option for each case. While this may be a good approach to discriminate among floorplans, an algorithm like this does not effectively learn to generate

a floorplan. *Chipformer*, [19] shows promising results in learning transferable policy placement through offline training and online fine-tuning of a decision transformer. This method improves efficiency compared to previously published works.

B. RL and Decision Transformers

Reinforcement learning is a type of machine learning where an agent learns to make decisions by performing actions in an environment to achieve a goal. In RL, the environment represents the problem or the space in which the agent operates. It manages the state, action, and reward transitions of the problem the agent is trying to solve. The agent improves its policy through its interaction with the states and rewards returned by the environment. More specifically, at each timestep, the agent selects an action (such as where to place a module) and the environment returns a reward (such as wirelength) for the action chosen and the next state. The objective is to learn a policy, $\pi^*(a|s)$, that learns to select an action given a state which maximizes the cumulative reward over time.

A cornerstone of RL is the action-value function [24]. Otherwise known as the Q-function, $Q^\pi(s, a)$ under policy π , is the expected return after taking an action a in state s and then following policy π :

$$Q^\pi(s, a) = \mathbb{E} \left[\sum_{k=0}^{\infty} \kappa^k R_{t+k+1} \mid S_t = s, A_t = a \right].$$

Typically, this Q-function is parameterized by some estimator (typically a neural network), giving us $Q_\theta^\pi(s, a)$. Similarly, the policy π is also parameterized by some estimator, π_θ . The agent interacts with the environment using its policy, and the Q-function guides the agent by estimating the value of actions. In actor-critic algorithms, this setup is formalized by having two distinct components: the actor and the critic.

The actor is responsible for selecting actions based on the current policy. It maps states to actions in a way that aims to maximize the expected cumulative reward. The policy $\pi_\theta(a | s)$ is learned through gradient ascent on the expected reward. The critic evaluates the actions taken by the actor by estimating the Q-function. It provides feedback on how good the actions are, which in turn helps the actor to improve its policy [16]. The critic learns to approximate the Q-function $Q_\theta^\pi(s, a) \approx Q^\pi(s, a)$, often using temporal difference learning, where the value estimates are updated based on the observed rewards and the estimated values of subsequent states [24].

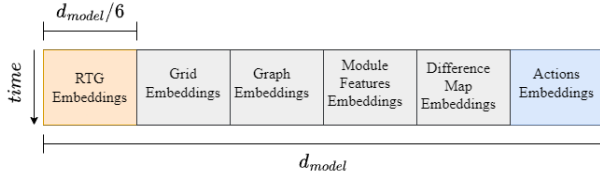


Fig. 2: The shape and positions of the input embeddings as they are placed in the *token embeddings*. We also add a time-wise positional embedding to the entire token (not shown). Note that we differ from existing work by considering this entire d_{model} -sized token embedding for a single timestep. Other work typically discretizes *states*, *actions*, *rewards* into sub-timesteps.

Decision transformers (DTs) [5] extend auto-regressive (causal) transformers [26] to decision-making problems. The idea is to learn offline from *trajectories*, Γ , and the *rewards-to-go*, g , where

$$\Gamma = \{(s_0, a_0, r_0), (s_1, a_1, r_1), \dots, (s_T, a_T, r_T)\},$$

and

$$g_t = \sum_{m=t}^T r_{m+1}.$$

In other words, g_t is the cumulative future rewards that the agent aims to achieve from a given timestep until the end of the trajectory. We use the subscript γ_t to denote the *trajectory-so-far*, which includes the states, actions, and rewards/rewards-to-go (SARs) seen up until t . This corresponds with $\Gamma[0 : t - 1]$ ¹.

The idea is to “prompt” the model into producing the desired actions in an auto-regressive manner. At the first timestep, the model is given a target cumulative reward value, which is the reward we aim to achieve after all decisions have been made. For each subsequent timestep: $\hat{a} = \text{DT}(\gamma_t, g_t)$, and the loss is computed between \hat{a} and a_t . Note that g_t is computed by subtracting the rewards the agent has seen so far from the target reward.

Online DT training works similarly. Trajectories are collected on policy in a replay buffer, and the likelihood of their occurrence is maximized using a max-entropy sequence

¹We slightly abuse notation here. For the actor, we time-delay all the actions by one step. In other words, the actor would see all actions up until a_{t-1} , but would see s_t and g_t . We forgo this time-shifting for the critic, as the critic is used to predict the return-to-go for $\pi(s_t, a_t, g_t)$.

modeling loss. For brevity, we refer readers to [29] for more details.

C. Reasoning in Structured Large Discrete Action Spaces

The floorplanning task involves placing various functional blocks on an integrated circuit to optimize multiple design criteria such as wirelength, congestion, and thermal performance. Each block can occupy numerous potential positions, leading to a combinatorial explosion of possible configurations. This interdependence and the vast number of possible placements make traditional reinforcement learning methods inefficient for such problems. To make things even worse, existing approaches are constrained by how they discretize the floorplan canvas². For example, a canvas discretized to 100×100 must have a linear layer of size 10^4 *just to inference*. If we were to make this canvas 3D with two layers, then our ML model would necessitate a linear layer of shape 2×10^4 . Just the size of these action spaces can make ML models too large to run many hardware configurations. Hardware concerns aside, the extreme size of the action space can make ordinary RL approaches not very sample efficient [4], [8].

To ameliorate this issue, we observe that floorplanning operates on a structured large discrete action space (SLDAS). A SLDAS is a discrete action space which can exhibit a form of structure known as *L action similarity* [2]. *L* action similarity is given by

$$L = \sup_{\substack{a, a' \in A' \\ a \neq a'}} \frac{|Q^\pi(s, a) - Q^\pi(s, a')|}{\|a - a'\|_2}$$

ensuring that

$$|Q^\pi(s, a) - Q^\pi(s, a')| \leq L \|a - a'\|_2 \quad \text{for all } a, a' \in A'.$$

The Wolpertinger agent [8] addresses these challenges by exploiting action similarity. By combining continuous action embeddings with k -nearest neighbor search, the agent is able to operate in a continuous domain while ensuring that selected actions are valid discrete placements. The consequence of this design choice is that the output shape of the model is no longer tied to the size of the action space. So for a 3-D floorplan, our output shape is 3, which corresponds with x, y, z placement locations in floating-point representation. This is unlike existing work which outputs a probability distribution **over all possible locations** [19], [23]. The Wolpertinger agent balances exploration efficiency and placement accuracy, making it well-suited for the large structured discrete action space inherent in floorplanning tasks. To the best of our knowledge, there does not exist any literature extending this work to modern auto-regressive models.

²For our work, the canvas is where the elements are to be placed. Our approach reasons over a 3D canvas but often times we explain things in the 2D case for clarity.

III. LARGE REASONING MODELS

In this section, we describe our Dreamweaver’s architecture by discussing the relevant prior work that guided our design process. We follow by explaining how our model is trained and the philosophy behind our paradigm. The first question we address is *what is a large reasoning model?* We define LRM as auto-regressive models that are designed to make decisions over a large ($|\mathcal{A}| > 10^4$) action space. Prior work in floorplanning has not addressed this fundamental issue of a tremendously large action space nor have they exploited its structure. A key observation we make is that placing a module in location x, y, z is likely to give a similar return as placing a module in location $x + \epsilon, y + \epsilon, z + \epsilon$. In other words, by considering a neighborhood near a proposed action rather than a single specific action, the model learns more efficiently.

A. Dreamweaver Architecture

Our model is composed of three fundamental blocks: the actor π_θ , the critic g_θ^π , and k -NN [10]. We first explain how the outputs of the components are fed into each other; we explain the specifics of the inputs to each component afterward. The actor is a causal-transformer [5], [26] which outputs the $\alpha_t = x, y, z$ floating-point coordinates of where it believes a particular macro should be placed. By doing this, we are able to decouple the output shape of our model from the floorplan canvas shape.

These proposed actions are then input into the k -NN module which returns the k closest (and valid) actions to what the actor proposed. The intention behind this step is two-fold. First, it discretizes the floating-point coordinates into the integers that correspond with locations on the canvas. Second, it allows us to mask out actions which are impermissible (placing one module in the same location as another, placing module out of the canvas).

Afterward, these k actions are fed into the critic. Figure 1 shows this flow of information. The critic is also a causal transformer and predicts the return to go of the k candidate actions. The action which most closely achieves the target g_t is ultimately selected. That is, we select:

$$\hat{a}_t = \arg \min_{a_t \in \{a_t^1, a_t^2, \dots, a_t^k\}} (g_\theta^\pi(a_t, \gamma_t) - g_t) \quad (1)$$

The output shape of both the actor and critic is 3. However, their activation functions differ. For the actor, we scale all $\alpha = \hat{x}, \hat{y}, \hat{z}$ coordinates between 0.0 and 1.0 via $0.5 \times (\tanh(\text{actor_logits}) + 1)$. In our case, due to all returns-to-go being positive, the critic’s logits are activated via $\text{ReLU}(\text{critic_logits})$ [1].

The three key inputs to the actor and critic are *RTGs*, *states*, and *actions*. Table I shows the encoding methods for the different inputs and figure 2 shows how they are embedded as tokens for both causal transformers. There are four components to the state:

- 1) **Grid.** This contains two features, the first feature is the locations of the already placed modules (the canvas).

This somewhat resembles figure 4. Inspired by the authors of Chipformer, the second feature shows the wirelength increases for placing a module at a particular location.

- 2) **Graph.** The netlists which define the modules and their interconnections are converted into a graph which is processed by a graph attention network [27]; specifically, at each timestep, we encode the difference between the graph that has been placed on the canvas so far and the overall graph which represents the netlist. We extract the **ModuleFeatures** from the netlist and use them as node features for the graph embeddings. Mathematically, the graph embedding at each timestep:

$$\mathcal{G}(t)_{\text{embed}} = \text{GAT}(\mathcal{G}_{\text{netlist}}(t)) - \text{GAT}(\mathcal{G}_{\text{placed}}(t)) \quad (2)$$

Note that our environment provides $\mathcal{G}_{\text{placed}/\text{netlist}}(t)$ and the actual GAT module resides within Dreamweaver.

- 3) **ModuleFeatures.** The module features relevant to making the placement decision are the height, width, area, and the *degree*, the number of connections to the module.
- 4) **DifferenceMap.** The difference map measures the change in the floorplan canvas across two consecutive timesteps.

The RTG encoder uses scaled dot product attention [26] to embed g_t ; we discuss this decision in more detail in table I and show the impact of this encoding mechanism in figure 3. The actions correspond with the x, y, z coordinates chosen so far for the already placed modules. Note that, for the critic, we append the k candidate actions returned by k -NN across the batch-axis and duplicate all the state and RTG information. This allows us to compute equation 1 to select the current timestep’s action. All the embedding mechanisms have an output shape of $\frac{1}{6} \cdot d_{\text{model}}$ as depicted in figure 2. Our $d_{\text{model}} = 288$, with 4 attention layers and 4 heads. We set the context length to $n_{\text{modules}} + 1$; we use the same parameters for both the actor and critic.

B. Training: Learning from Random Floorplans

Dreamweaver learns to make decisions via offline training. However, in order to perform offline training, we would typically need expert trajectories $\Gamma^* \sim \pi^*$ which emulates the decision-making of an optimal policy. This is problematic because this necessitates either human experts to construct a dataset of trajectories or we must use an existing floorplanning tool which we would treat as an “expert.” Chipformer takes the latter approach by harnessing the outputs of MaskPlace [20] to create $\hat{\Gamma}^*$.

However, for various reasons, obtaining an expert trajectory dataset can be infeasible or intractable. Especially in the case of floorplanning, verifying that a given floorplan trajectory is optimal cannot be done efficiently unless $P = NP$. This is a direct consequence of the floorplanning being NP-hard. For this reason, we forgo collecting an expert trajectory dataset and **train on entirely random trajectories**, Γ_ξ .

We obtain Γ_ξ by randomly selecting a legal action from our floorplanning environment at each timestep and storing the

resulting states and rewards. Note that the goal of doing this is **not** because we are hoping we will at some point randomly produce a perfect floorplan, but because we want to learn *the consequences of actions*.

Our actor is trained by minimizing:

$$L_{DWActor} = \|a_\Gamma - a_t\|_1 \quad (3)$$

where $a_t = \pi_\theta(\gamma)$; our actor is trained to match the actions of the trajectory given γ . Analogously, the critic is trained to minimize the error in predicting the return to go:

$$L_{DW Critic} = \|g_\Gamma - g_\theta(\gamma)\|_1 \quad (4)$$

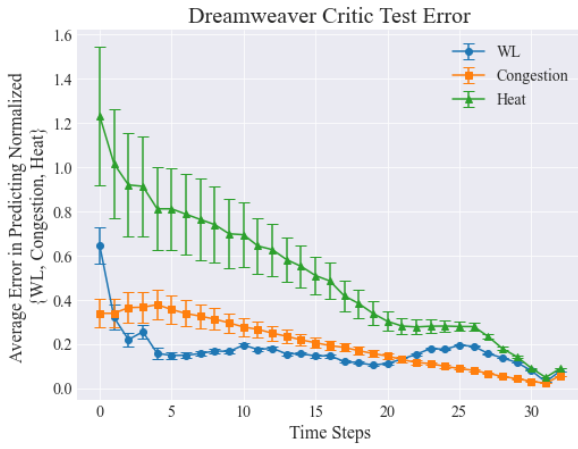


Fig. 3: Our environment returns three proxy metrics at each timestep, t : wirelength (WL), congestion and thermals. This chart shows the Dreamweaver critic’s error in estimating the RTG with respect to γ_t . Error bars show variance over the trajectories.

The rationale behind training on random trajectories is many-fold. The first reason can be summed up by Thomas Edison’s famous quote:

I have not failed. I’ve just found 10,000 ways that won’t work.

A much more formal perspective is given by hindsight experience replay (HER) and goal-conditioned supervised learning (GCSL) [3], [11]. The idea behind HER and GCSL is to consider failed attempts as valuable learning experiences by relabeling the trajectories to be optimal in hindsight as though the data came from an optimal agent with a different goal. However, their loss is for categorical action spaces:

$$L_{JGCSL}(\pi) = -\mathbb{E} \left[\sum_{t=0}^T \log \pi(a = a_t | \gamma_t) \right]. \quad (5)$$

This loss computes the maximum-likelihood estimate of a_t given γ_t . In order to work in a continuous action space, we need to modify this objective. If we assume that the errors follow a Laplace distribution, the maximum likelihood estimate becomes $L_{DWActor}$ [25]. An analogous mapping

can be done between $L_{DW Critic}$ and HER. In summary, the training procedure of our algorithm can be thought of as a form of GCSL to train the actor and HER being used to train the critic.

By training on a diverse set of random trajectories, our model can learn from a wide variety of scenarios, leading to better generalization. This comes in handy because in floorplanning, oftentimes reducing wirelength has the negative consequence of worsening thermals and congestion [13], [18]; so learning a diversity of designs can be of practical benefit.

Another practical reason is the computational feasibility; generating random trajectories is straightforward and does not require the costly process of acquiring expert knowledge. Furthermore, this approach allows users to leverage existing drafts of floorplans that have already been evaluated for metrics. In other words, this approach addresses sample efficiency from another direction; we permit normally “sub-optimal” samples to help us. Other work in RL has also remarked on the importance of sub-optimal trajectories. For example, the authors of *Multi-Game DTs* have found that incorporating non-expert trajectories into training improved performance [21].

IV. EXPERIMENTS

In this section, we describe the comparisons made against the current SOTA, Chipformer [19]. To do this, we go over the RL environment which handles the state-action-reward dynamics of our agents, and describe the experiments we run. The appendix contains the modifications made to adapt Chipformer for our tasks.

A. RL Environment

For our experiments, we produce an RL environment that works with the MCNC benchmark [17]. To do this, we configure our environment to return the states listed in III-A. For the rewards, we address the multi-objective nature of floorplanning by returning three values at each timestep. $R_t = (w_t, c_t, h_t)$ which correspond with a wirelength score (\uparrow), congestion penalty (\downarrow) and thermals penalty (\downarrow). The wirelength score is a proxy for the 3D Manhattan wirelength so far; the score increases inversely with wirelength. Because we are working in 3D, we impose a “via penalty” by multiplying z-axis distances by 10. We estimate congestion via a simple 3D convolutional density estimation kernel. Thermals are estimated similarly to congestion, but we weigh modules with more connections as having greater heat output. We omit the granular details of these estimates as these estimates could be generic proxies of floorplan performance metrics, while wirelength is the dominating metric in this study.

In addition to states and returns, our environment also returns two auxiliary pieces of information. The first is the current module and orientation to be placed; to pick these, we follow [19], [23] by selecting the largest area modules and selecting the orientation by picking the option with the maximum number of legal actions at each timestep. The second auxiliary detail is a mask which is the shape of the canvas, that marks which locations are legal-illegal.

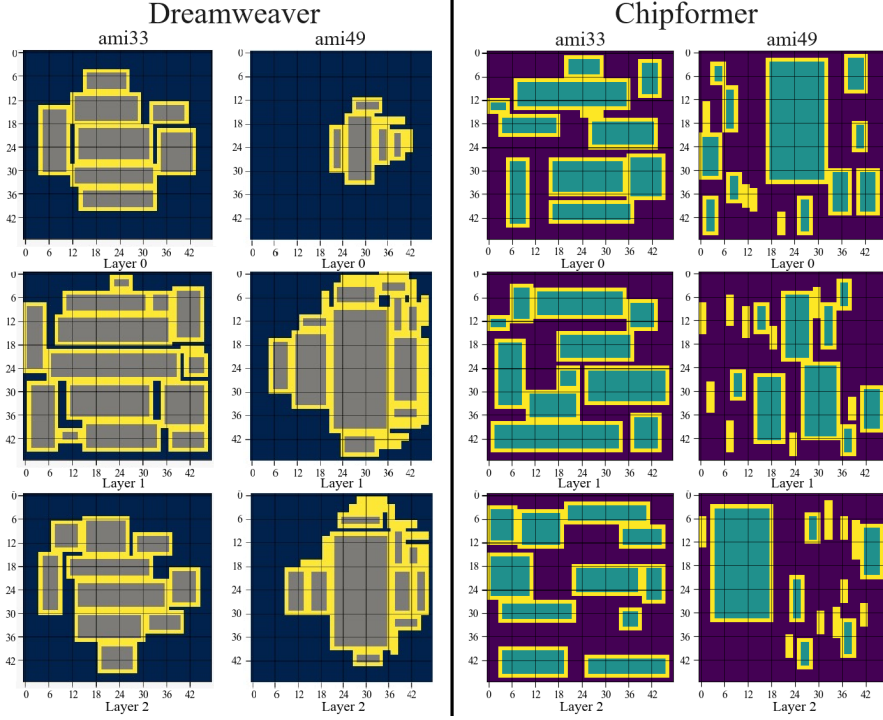


Fig. 4: The following shows 3-layer floorplans generated from the *ami33* and *ami49* netlists. The total Manhattan wirelength (\downarrow) of Dreamweaver is 200,738 and 28,636 as opposed to 225,877 and 39,442 of Chipformer for the aforementioned netlists, respectively. The lower wirelength for *ami49* can be explained by the latter having significantly fewer connections compared to *ami33*. Note that Chipformer was trained offline and fine-tuned online whereas Dreamweaver was trained offline.

B. Evaluations

As stated earlier, we acknowledge that modern floorplans must consider metrics such as thermals and congestion in addition to wirelength. However, to maintain parity with Chipformer, we perform an experiment on the *ami33* and *ami49* netlists from the MCNC dataset where we only consider optimizing wirelength. To do this, we prepared $|\Gamma_\xi| = \{510, 200\}$ for *ami33* and *ami49* respectively. Additionally, for Chipformer, we prepared a random warm-up trajectory buffer initialized to $\Gamma_{\text{online}} \leftarrow \Gamma_\xi$ with $|\Gamma_\xi| = 60$ for both netlists.

Chipformer was trained offline for 2000 epochs for both benchmarks. Following this, it was further fine-tuned via online training. The online training was done on Γ_{online} for 5 iterations, 10 rollouts per iteration, and 50 epochs per rollout. For both offline and online training, we used the AdamW($\eta = 6e - 4$) optimizer [22]. Values for their parameters, β and λ , were selected to improve performance and maintain a certain level of exploration in their loss function. For *ami33*, both β and λ were set to 0.5. Both of these values were updated to 0.7 for *ami49* as they improved Chipformer's performance.

For both netlists, Dreamweaver was trained offline on the same randomly generated trajectories as Chipformer. The model was trained for a total of 300 epochs using AdamW($\eta = \{5e - 4, 5e - 3\}$) for the actor and critic, respectively. For inferencing, the following variables allow us to explain how Dreamweaver's target reward was selected. Let

$\mu_\gamma = (\mu_w, \mu_c, \mu_h)$ and $\sigma_\gamma = (\sigma_w, \sigma_c, \sigma_h)$ represent the mean and standard deviation of the returns of Γ_ξ . We prompt our model with $(\mu_w + 3\sigma_w, \mu_c, \mu_h)$. For both netlists, we had Dreamweaver and Chipformer inference three times and we took the best result.

We perform a second experiment to measure the critic's accuracy in estimating the RTG at each timestep. The goal of this experiment is to determine how well the critic performs at predicting the final performance of a floorplan, given γ_t . To do this, we trained our model as we did for the wirelength experiment and then had the critic inference on 30 unseen trajectories from *ami33*. At each timestep, the critic predicts the return to go based on the trajectory so far.

V. RESULTS AND DISCUSSION

This work introduces large reasoning models, a variation of auto-regressive models capable of reasoning over large action spaces. Dreamweaver leverages the actor-critic architecture to learn the relationships among the different metrics of an IC floorplan, e.g. wirelength, thermals, and congestion, and tries to optimize the layout over a 3D canvas. The performance of the model (without fine-tuning) was evaluated on the *ami33* and *ami49* benchmarks and compared against the state-of-the-art offline trained and online fine-tuned Chipformer. In both scenarios, Dreamweaver showed superior performance in minimizing the wirelength.

Additionally, Dreamweaver decouples the output dimension of large action spaces by combining continuous action embeddings with k -nearest neighbor search and thus breaks free of the ‘heavy computational resource requirement’ norm plaguing most contemporary works.

Moreover, it should be emphasized that this model learns to generate floorplans without requiring expert data via GCSL—a point that can have deep implications for reducing the manufacturing costs of electronic devices. Not to mention, this actor-critic framework permits us to use the critic outside the context of decision-making. For example, the critic can be a stand-alone estimator for the return-to-go for a partially complete floorplan.

An interesting interpretation of the critic’s performance can be made from figure 3. The decreasing variance represents the perplexity of the critic going down with every timestep. This aligns with our understanding of natural language processing in a sense similar to predicting the next word in the sentence given the sentence so far. We can argue that as more modules are placed on the canvas, the uncertainty of the change in wirelength, thermals, or congestion will usually decay.

However, Dreamweaver still leaves room for improvement—further complexities of the floorplanning process have to be considered before this is approved for industrial use. The appendix contains a thorough discussion on our limitations.

REFERENCES

- [1] Abien Fred Agarap. Deep learning using rectified linear units (relu). *arXiv preprint arXiv:1803.08375*, 2018.
- [2] Fabian Akkerman, Julius Luy, Wouter van Heeswijk, and Maximilian Schiffer. Handling large discrete action spaces via dynamic neighborhood construction. *arXiv preprint arXiv:2305.19891*, 2023.
- [3] Marcin Andrychowicz, Filip Wolski, Alex Ray, Jonas Schneider, Rachel Fong, Peter Welinder, Bob McGrew, Josh Tobin, OpenAI Pieter Abbeel, and Wojciech Zaremba. Hindsight experience replay. *Advances in neural information processing systems*, 30, 2017.
- [4] Yash Chandak, Georgios Theοcharous, James Kostas, Scott Jordan, and Philip Thomas. Learning action representations for reinforcement learning. In *International conference on machine learning*, pages 941–950. PMLR, 2019.
- [5] Lili Chen, Kevin Lu, Aravind Rajeswaran, Kimin Lee, Aditya Grover, Misha Laskin, Pieter Abbeel, Aravind Srinivas, and Igor Mordatch. Decision transformer: Reinforcement learning via sequence modeling. *Advances in neural information processing systems*, 34:15084–15097, 2021.
- [6] Ruoyu Cheng and Junchi Yan. On joint learning for solving placement and routing in chip design. *Advances in Neural Information Processing Systems*, 34:16508–16519, 2021.
- [7] Vladimir G Deineko and Gerhard J Woeginger. Complexity and approximability results for slicing floorplan designs. *European Journal of Operational Research*, 149(3):533–539, 2003.
- [8] Gabriel Dulac-Arnold, Richard Evans, Hado van Hasselt, Peter Sunehag, Timothy Lillicrap, Jonathan Hunt, Timothy Mann, Theophane Weber, Thomas Degris, and Ben Coppin. Deep reinforcement learning in large discrete action spaces. *arXiv preprint arXiv:1512.07679*, 2015.
- [9] Matthias Fey and Jan E. Lenssen. Fast graph representation learning with PyTorch Geometric. In *ICLR Workshop on Representation Learning on Graphs and Manifolds*, 2019.
- [10] Evelyn Fix. *Discriminatory analysis: nonparametric discrimination, consistency properties*, volume 1. USAF school of Aviation Medicine, 1985.
- [11] Dibya Ghosh, Abhishek Gupta, Ashwin Reddy, Justin Fu, Coline Devin, Benjamin Eysenbach, and Sergey Levine. Learning to reach goals via iterated supervised learning. *arXiv preprint arXiv:1912.06088*, 2019.
- [12] Virginia Martín Hériz, Je-Hyoung Park, Travis Kemper, Sung-Mo Kang, and Ali Shakouri. Method of images for the fast calculation of temperature distributions in packaged vlsi chips. In *2007 13th International Workshop on Thermal Investigation of ICs and Systems (THERMINIC)*, pages 18–25. IEEE, 2007.
- [13] Hsin-Hsiung Huang, Chung-Chiao Chang, Chih-Yuan Lin, Tsai-Ming Hsieh, and Chih-Hung Lee. Congestion-driven floorplanning by adaptive modular shaping. In *48th Midwest Symposium on Circuits and Systems*, 2005, pages 1067–1070 Vol. 2, 2005.
- [14] Andrew B. Kahng. Classical floorplanning harmful? In *Proceedings of the 2000 International Symposium on Physical Design*, ISPD ’00, page 207–213, New York, NY, USA, 2000. Association for Computing Machinery.
- [15] Thomas N Kipf and Max Welling. Variational graph auto-encoders. *arXiv preprint arXiv:1611.07308*, 2016.
- [16] Vijay Konda and John Tsitsiklis. Actor-critic algorithms. *Advances in neural information processing systems*, 12, 1999.
- [17] K. Kozminski. Benchmarks for layout synthesis - evolution and current status. In *28th ACM/IEEE Design Automation Conference*, pages 265–270, 1991.
- [18] S.T.W. Lai, E.F.Y. Young, and C.C.N. Chu. A new and efficient congestion evaluation model in floorplanning: wire density control with twin binary trees. In *2003 Design, Automation and Test in Europe Conference and Exhibition*, pages 856–861, 2003.
- [19] Yao Lai, Jinxin Liu, Zhentao Tang, Bin Wang, Jianye Hao, and Ping Luo. Chipformer: Transferable chip placement via offline decision transformer. In *International Conference on Machine Learning*, pages 18346–18364. PMLR, 2023.
- [20] Yao Lai, Yao Mu, and Ping Luo. Maskplace: Fast chip placement via reinforced visual representation learning. *Advances in Neural Information Processing Systems*, 35:24019–24030, 2022.
- [21] Kuang-Huei Lee, Ofir Nachum, Mengjiao Sherry Yang, Lisa Lee, Daniel Freeman, Sergio Guadarrama, Ian Fischer, Winnie Xu, Eric Jang, Henryk Michalewski, et al. Multi-game decision transformers. *Advances in Neural Information Processing Systems*, 35:27921–27936, 2022.
- [22] Ilya Loshchilov and Frank Hutter. Decoupled weight decay regularization. *arXiv preprint arXiv:1711.05101*, 2017.
- [23] Azalia Mirhoseini, Anna Goldie, Mustafa Yazgan, Joe Wenjie Jiang, Ebrahim Songhori, Shen Wang, Young-Joon Lee, Eric Johnson, Omkar Pathak, Azadeh Nazeri, et al. A graph placement methodology for fast chip design. *Nature*, 594(7862):207–212, 2021.
- [24] Richard S Sutton and Andrew G Barto. *Reinforcement learning: An introduction*. MIT press, 2018.
- [25] Harry L Van Trees. *Detection, estimation, and modulation theory, part I: detection, estimation, and linear modulation theory*. John Wiley & Sons, 2004.
- [26] Ashish Vaswani, Noam Shazeer, Niki Parmar, Jakob Uszkoreit, Llion Jones, Aidan N Gomez, Łukasz Kaiser, and Illia Polosukhin. Attention is all you need. *Advances in neural information processing systems*, 30, 2017.
- [27] Petar Veličković, Guillem Cucurull, Arantxa Casanova, Adriana Romero, Pietro Liò, and Yoshua Bengio. Graph attention networks, 2018.
- [28] Qi Xu, Hao Geng, Song Chen, Bo Yuan, Cheng Zhuo, Yi Kang, and Xiaojing Wen. Goodfloorplan: Graph convolutional network and reinforcement learning-based floorplanning. *IEEE Transactions on Computer-Aided Design of Integrated Circuits and Systems*, 41(10):3492–3502, 2022.
- [29] Qinqing Zheng, Amy Zhang, and Aditya Grover. Online decision transformer. In *international conference on machine learning*, pages 27042–27059. PMLR, 2022.

VI. APPENDIX

A. Model and Experiment Parameters

TABLE I: Input Encoding Mechanisms for the Actor and Critic

Input Name	Input Shape	Encoding Mechanism
Return-to-Go (RTGs)	[block_size, rtg_dim]	Linear(rtg_dim, n_embed) → MultiheadAttention(embed_dim = d_embed, n_heads = 4)
Grid	[block_size, 2, fp_layers, grid_size, grid_size]	Conv3d(2, 16, kernel_size = (3, 3, 3)) → ReLU() → Conv3d(16, 24, kernel_size = (3, 3, 3)) → ReLU() → Flatten() → Linear(24 × grid_size × grid_size × fp_layers, d_embed) → Tanh()
Graph	List of [n_timesteps, PYG Graph [9]]	GATConv(mod_feat_size, d_embed, heads = n_head)
Module Features	[block_size, mod_feat_size]	Linear(mod_feat_size, d_embed) → Tanh()
Difference Map	[block_size, 2, fp_layers, grid_size, grid_size]	Conv3d(2, 16, kernel_size = (3, 3, 3)) → ReLU() → Conv3d(16, 24, kernel_size = (3, 3, 3)) → ReLU() → Flatten() → Linear(24 × grid_size × grid_size × fp_layers, d_embed) → Tanh()
Actions	[block_size, action_dim]	Linear(action_dim, d_embed) → Tanh()
Timesteps	[block_size, 1]	Embedding Layer(output shape = d_{model})

The input shapes and encoding mechanisms are shown. The different layers used for the encoders are described along with the output shapes. We define $d_{embed} = d_{model}/6$. Note that we use multi-head attention to encode the RTG. The reason for doing this is because we want our model to understand *how* wirelength, thermals, and congestion influence one another. We hypothesize that by performing self-attention on these three returns over time, Dreamweaver will learn a more concrete representation of their interplay.

We measure the wirelength using the discretized floorplan (the canvas). That is to say, we compute the Manhattan distance between centroids $a, b \in \mathbb{R}^{48 \times 48 \times 3}$. Where Manhattan distance with a via-penalty of 10.0 is given by:

$$\text{dist}(a, b) = \mathcal{A}(a, b) \cdot (|a_x - b_x| + |a_y - b_y| + 10.0 \times |a_z - b_z|)$$

where a_x, a_y, a_z and b_x, b_y, b_z are the x, y, and z coordinates of centroids a and b , respectively. $\mathcal{A}(a, b)$ represents the number of connections between modules a and b .

TABLE II: Hyperparameters for Dreamweaver Actor and Critic

Hyperparameter	Actor & Critic
Number of attention layers	4
Number of attention heads	4
k (for k -NN)	5
Learning rate	{5e-4, 5e-3}
Optimizer	AdamW
d -model	288
Batch size	30
Number of epochs	300
Timesteps	34 (ami33), 50 (ami49)
Block size (block_size)	Timesteps
RTG dimension (rtg_dim)	3
Canvas shape	$48 \times 48 \times 3$
Canvas length and width (grid_size)	48
Canvas layers (fp_layers)	3
Module feature dimension (mod_dim_size)	4
Action dimension (action_dim)	3

B. Limitations

Like analytical and metaheuristic methods, our method does not entirely address the complexities of floorplanning. The floorplan model of this study assumes a fixed floorplan canvas area, which does not permit area optimization for the dies in a single setting. In addition, the outline of all the design modules are assumed to be fixed rectangular shapes, this was shown to be overly constraining for modern IC designs [14]. Performance metrics such as optimization for power and frequency domains are also overlooked. Currently, additional placement constraints on modules, such as placement constraints for the interface modules, and clustering for power delivery network (PDN) optimization, are not often included in automated floorplanning studies. However, they are crucial for practical applications. We are looking forward to considering these aspects in future work.

Another concern revolves around the thermal estimations of the stack. Given that our floorplanning benchmark does not include data on power dissipation, we generated a surrogate value for each module based on the connectivity. In our setup, we employ a convolutional kernel to estimate temperature by analyzing the power density of the floorplan within a 3D window, with the module's power intensity serving as an indicator of temperature. While such heuristics are not uncommon, there is room for improvement in this approach [12].

C. Adapting Chipformer for 3D Placement

For our experiments, we compare against Chipformer, the current state of the art. Due to our experiments involving 3D floorplanning, we had to adjust Chipformer in various ways to adapt it to our setup. We followed the author's implementation when possible and made reasonable adjustments. The changes we made are:

- 1) Their work originally encoded the grid using 2DConv layers. We update this to 3DConv to support the 3D canvas.
- 2) Their transformer is typically configured with 6 attention layers, 8 heads and $d_{model} = 128$. We keep all of these the same but set $d_{model} = 140$ to allow for greater expressive capability due to the 3D canvas. Furthermore, we set their context length to $n_modules + 1$ because this is equivalent to the maximum number of timesteps.
- 3) We use a graph auto-encoder (GAE) rather than a variational graph auto-encoder as we found this improved their performance [15].
- 4) Similar to figure 2, we consider an entire SAR as a single timestep rather than a *state*, *action* and *reward* becoming separate sub-timesteps. We did this by concatenating the circuit token, grid token, action token and (empty) RTG token into a single token embedding of size d_{model} , with each of the aforementioned tokens having size $d_{model}/4$.

We do not modify their offline and online training paradigms—we use their return-guided prioritization weight and the same hyperparameters as they recommend unless we state differently. We create their “circuit token” from netlists in the MCNC benchmark via the GAE and use these for offline training. Note that Chipformer does not use RTGs as inputs to their model. Afterward, we allow the model to learn online using their max-entropy sequence loss with a return-guided prioritization weighting scheme.